

Remote sensing reflectance


VERSION	v1.2
RELEASE DATE	Aug 20th, 2024
KEYWORDS	OCEAN COLOR Under: EARTH SCIENCE > OCEANS > OCEAN OPTICS
CREATORS	Amir Ibrahim, Bryan Franz, Sean Bailey, Jeremy Werdell, Zia Ahmad, and Curtis Mobley
EDITORS	Amir Ibrahim and Bryan Franz
DOI	10.5067/FQBB0C1K43OJ 

Table of Contents

Abstract

Plain Language Summary

Version description

1. Introduction

2. Context / Background

2.1. Historical Perspective

2.2. Additional information

3. Algorithm Description

3.1. Scientific Theory

3.1.1. Assumptions

3.2. Mathematical Theory

3.2.1. Assumptions

3.3. Algorithm Input Variables

3.4. Algorithm Output Variables

4. Algorithm Availability

4.1. Location of Implemented Algorithm #1

5. Algorithm Usage Constraints

6. Performance Assessment Validation

6.1. Performance Assessment Validation Methods

6.2. Performance Assessment Validation Uncertainties

6.3. Performance Assessment Validation Errors

7. Data Access

7.1. Input Data Data Access

7.1.1. Entry #1

7.2. Output Data Data Access

7.2.1. Entry #1

7.3. Important Related URLs

7.3.1. Entry #1

8. Contacts

References

Abstract

The atmospheric correction algorithm calculates the spectral "remote sensing" reflectance, $R_{rs}(\lambda)$, from beneath the ocean surface, normalized by the solar irradiance falling on it, crucial for deriving data from ocean color sensors. $R_{rs}(\lambda)$, expressed in steradians^{-1} , serves as the primary input for various oceanic measurements such as chlorophyll-a concentration, water's diffuse attenuation, and inherent optical properties. The algorithm also retrieves atmospheric aerosol properties, including aerosol optical depth (AOT) and angstrom exponent (α), offering insights into the algorithm's performance. These products form part of the standard Level-2 and Level-3 ocean color data suites, applicable across all current ocean color sensors. The Multi-band Atmospheric Correction (MBAC) algorithm leverages hyperspectral information for improved atmospheric correction, is utilized for PACE OCI, and will be utilized for future reprocessing of heritage ocean color missions.

Plain Language Summary

No content available.

Version description

This is the first APT version of the atmospheric correction algorithm employed by the Ocean Biology Processing Group (OBPG). Previous ATBD information for this algorithm was provided by the OBPG through the Ocean Biology Distributed Active Archive Center (OB.DAAC) website. This version describes the algorithm as implemented in the most recent PACE OCI data processing.

1. Introduction

This algorithm derives the spectral radiance upwelling from beneath the ocean surface, normalized by the downwelling solar irradiance and expressed as spectral "remote sensing" reflectance, $R_{rs}(\lambda)$ at each sensor wavelength, λ , in the visible domain with units of sr^{-1} . $R_{rs}(\lambda)$ is the fundamental quantity to be derived from ocean color sensors, as it provides the basic input to many derived product algorithms such as chlorophyll-a, diffuse attenuation, or inherent optical properties. A by-product of the $R_{rs}(\lambda)$ derivation is the retrieved atmospheric aerosol optical properties of aerosol optical depth (AOT; dimensionless) and aerosol angstrom exponent (α ; dimensionless). These aerosol properties provide a diagnostic on algorithm performance. The $R_{rs}(\lambda)$ algorithm is applicable to all current ocean color sensors. The $R_{rs}(\lambda)$ and associated AOT and α products are included as part of the standard Level-2 OC product suite and the Level-3 RRS product suite.

2. Context / Background

2.1. Historical Perspective

The development of atmospheric correction began in earnest with the launch of the Coastal Zone Color Scanner (CZCS) in 1978 on the Nimbus-7 satellite. As the first sensor designed specifically for observing ocean color, CZCS represented a pioneering step. However, the early years were challenging, as the atmospheric correction methods available were basic and often inadequate for dealing with the complexity of atmospheric conditions and aerosol types, due to the limitation of spectral bands. The 1990s saw substantial progress with the advent of the Ocean Color and Temperature Scanner (OCTS) and the Sea-Viewing Wide Field-of-View Sensor (SeaWiFS), launched in 1996 and 1997, respectively. These sensors benefited from improved technology and a deepening understanding of atmospheric interactions. An important development of this era was the atmospheric correction algorithm introduced by Howard Gordon and Menghua Wang, which became foundational for the field Gordon & Wang, 1994. This algorithm, which utilized near-infrared (NIR) bands to estimate and remove atmospheric aerosol effects, is known as the black pixel assumption due to significant water absorption. In 2010, the algorithm was then combined with the NIR iterative approach to better model ocean reflectance in turbid waters, where the black pixel assumption is violated Bailey et al., 2010-03. Additionally, a new set of aerosol models was developed based on

inferred aerosol microphysical properties from the Aerosol Robotic Network (AERONET) observations. The 80 aerosol models by Ahmad et al., 2010 allowed for additional flexibility in selecting the aerosol types and provided more accurate aerosol products necessary for atmospheric correction. Finally, in 2019, the Multi-band Atmospheric Correction (MBAC) algorithm was developed to better utilize the additional spectral information that hyperspectral ocean color sensors offer in the NIR and Shortwave Infrared (SWIR) bands Ibrahim et al., 2019.

2.2. Additional information

No content available.

3. Algorithm Description

3.1. Scientific Theory

The fundamental quantity to be derived from ocean color sensors is the spectral distribution of reflected visible solar radiation upwelling from below the ocean surface and passing through the sea-air interface. Spaceborne ocean color sensors, however, measure the spectral radiance exiting the top of the atmosphere (TOA). The majority of that observed TOA radiance is light reflected by air molecules and aerosols within the atmosphere, and those contributions must be accurately modeled and removed from the observed signal. Similarly, surface contributions from whitecaps and sun glint, the specular reflection of the sun into the sensor field of view, must be estimated and removed. Finally, the attenuating effects of absorbing atmospheric gases and scattering losses due to transmittance of the water-leaving radiance through the atmosphere must be corrected. The process of retrieving water-leaving radiance from TOA radiance is typically referred to as atmospheric correction.

3.1.1. Assumptions

The total radiance L_t measured by a satellite-borne sensor at the top of the atmosphere (TOA) is assumed to come from contributions by atmospheric scattering, L_{atm}

; Sun and sky radiance reflected back upward by the sea-surface and reaching the TOA, L_{surf}^{TOA} ; and water-leaving radiance that reaches the TOA, L_w^{TOA} :

$$L_t = L_{atm} + L_{surf}^{TOA} + L_w^{TOA} \quad (1)$$

For brevity, the viewing direction (θ_v, ϕ_v) and wavelength λ are not shown. Expanding this equation into further levels of detail requires the definition of many different radiances, and precise notation is needed. The atmospheric contribution L_{atm} is always considered to be at the TOA. However, the surface-reflected radiance and water-leaving radiance can be formulated either at the sea surface or at the TOA. For these radiances, a superscript TOA will be used to specify the TOA value. Thus L_w will denote the water-leaving radiance just above the sea surface, and L_w^{TOA} will denote how much of L_w reaches the TOA.

3.2. Mathematical Theory

The retrieved water-leaving radiances, $L_w(\lambda)$, at each sensor wavelength, λ , are then normalized to remove remaining effects of solar geometries and atmospheric attenuation of the downwelling radiation to produce normalized water-leaving radiance, $nL_w(\lambda)$, which is often expressed as a radiance reflectance, $R_{rs}(\lambda)$ or Remote Sensing Reflectance, by simply dividing by the mean extraterrestrial solar irradiance, $F_0(\lambda)$.

In this algorithm, the TOA radiance is assumed to be partitioned linearly into various distinct physical contributions as shown below:

$$L_t(\lambda) = [L_r(\lambda) + [L_a(\lambda) + L_{ar}(\lambda)] + t_{d_v}(\lambda)L_f(\lambda) + t_{d_v}(\lambda)L_w(\lambda)]t_{g_v}(\lambda)t_{g_s}(\lambda)f_p(\lambda) \quad (2)$$

where:

Table 1: Radiance and transmittance notation. Spectral radiance L has SI units of $\text{mW cm}^{-2} \mu\text{m}^{-1} \text{sr}^{-1}$ is used in NASA's processing.

Symbol	Definition
$L_r(\lambda)$	the radiance contribution due to Rayleigh scattering by air molecules
$L_a(\lambda)$	the contribution due to multiple scattering by aerosols

$L_{ar}(\lambda)$	the contribution due to aerosol-molecule multiple scattering interactions
$L_f(\lambda)$	the contribution from surface whitecaps and foam
$L_w(\lambda)$	the water-leaving radiance component
$t_{d_v}(\lambda)$	the transmittance of diffuse radiation through the atmosphere in the viewing path from surface to sensor
$t_{d_s}(\lambda)$	the transmittance of diffuse radiation through the atmosphere in the viewing path from Sun to surface
$t_{g_v}(\lambda)$	the transmittance loss due to absorbing gases for all upwelling radiation traveling along the sensor view path
$t_{g_s}(\lambda)$	the transmittance of diffuse radiation through the atmosphere in the viewing path from Sun to surface
$f_p(\lambda)$	is an adjustment for effects of polarization sensitivity.

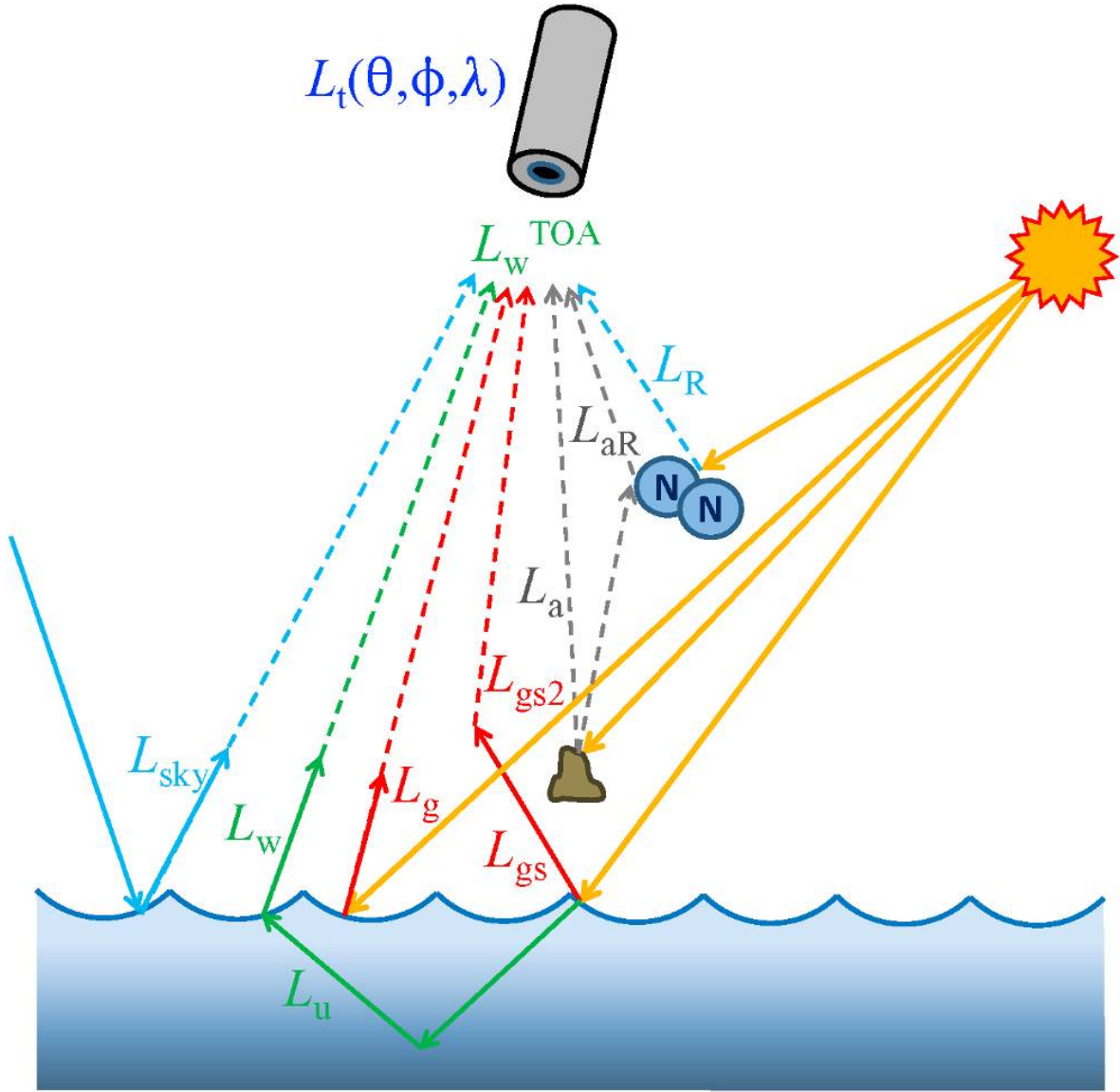


Figure 1: Qualitative illustrations of the various processes contributing to the total TOA radiance. The notation corresponds to Table 1.

The atmospheric correction algorithm retrieves $L_w(\lambda)$ by estimating and subtracting the terms on the right-hand side of the above equation from $L_t(\lambda)$. The $R_{rs}(\lambda)$ is then computed as:

$$R_{rs}(\lambda) = (L_w(\lambda) / (F_0 f_s \cos(\theta_s) t_{d_s})) f_b(\lambda) f_\lambda \quad (3)$$

where:

Table 2: Notations of variables to normalize the water-leaving radiance to compute

Symbol	Definition
F_0	extraterrestrial solar irradiance based on TSIS-1 Version 2 (Coddington et al. 2023)
f_s	adjustment of F_0 for variation in Earth-Sun distance
f_b	bidirectional reflectance correction
f_λ	correction for out-of-band response

Most of the terms in the above equations are estimated through precomputed radiative transfer simulations or models that depend only on the sensor spectral response, solar and sensor viewing geometry, and ancillary information such as atmospheric gas concentrations, surface windspeeds, and surface pressure. We utilize a successive order of scattering radiative transfer code by Zhai et al., 2009-02.

The primary challenge in ocean color atmospheric correction is the estimation of the aerosol contribution, as aerosols are highly variable and must be inferred from the sensor observations. The aerosol estimation follows the work of Ibrahim et al., 2019, with aerosol models detailed in (Ahmad et al. 2010). This algorithm relies on sensor observations from two bands in the near-infrared region (e.g., 748nm and 869nm for MODIS), where the water leaving radiance contributions are generally small and can be accurately estimated through an iterative bio-optical modeling approach as described in Bailey et al., 2010-03.

For a full description of the atmospheric correction algorithm, including details on the estimation of each term in the above equations and the operational process through which aerosol contributions are estimated and removed, the reader is referred to the document titled Atmospheric Correction for Satellite Ocean Color Radiometry and the associated Web Book on Atmospheric Correction. The web book was developed as an online resource for the theoretical basis and implementation of the current standard atmospheric correction algorithm employed by NASA for all ocean color missions, and it will be maintained as the algorithm evolves.

3.2.1. Assumptions

The algorithm makes several important assumptions:

1. There is no coupling between the upwelling underwater light field and the atmosphere.

2. The aerosol LUT is calculated for a flat ocean surface.
3. The aerosols are assumed to be spherical and weakly to non-absorbing.
4. There is no coupling between the gas absorption and aerosol and molecule scattering.

3.3. Algorithm Input Variables

Name	Long Name	Unit
rhot	Top of Atmosphere reflectance	sr ⁻¹
Pressure	Surface pressure	mbar
Humidity	Near surface relative humidity	%
Wind speed	Surface wind speed	m/s
Ozone	Column ozone concentration	Dobson Unit
Water vapor	Column water vapor concentration	cm
NO ₂	Nitrogen Dioxide	Dobson Unit
solz	Solar zenith angle	degree
relaz	Relative azimuth angle	degree
senz	Sensor zenith angle	degree

3.4. Algorithm Output Variables

Name	Long Name	Unit
R _{rs}	Spectral Remote Sensing Reflectance	sr ⁻¹
AOT	Aerosol Optical Thickness	No content available.

Name	Long Name	Unit
Angstrom	Angstrom exponent	No content available.

4. Algorithm Availability

4.1. Location of Implemented Algorithm #1

URL	https://oceancolor.gsfc.nasa.gov/docs/ocssw/atmcor2_8c_source.html
DESCRIPTION	The algorithm source code.

5. Algorithm Usage Constraints

Table 3: Algorithm implementation constraints

Product Short Name	Rrs_vv, where vv = sensor specific center wavelength in nm (see table below). Additional products associated with the Rrs retrieval algorithm are the aerosol angstrom exponent, angstrom, and the aerosol optical thickness, aot_nnn, where nnn is the longest aerosol selection band (see table below) and angstrom is the powerlaw exponent that relates aot_443 to aot_nnn.
Level-2 Product Suite	OC
Level-3 Product Suite	RRS
Level-3 Maskin	ATMFAIL, LAND, HILT, HISATZEN, STRAYLIGHT, CLDICE, COCCOLITH, LOWLW, CHLWARN, CHLFAIL, NAVWARN, MAXAERITER, ATMWARN, HISOLZEN, NAVFAIL, FILTER, HIGLI

The table below lists the sensor-specific center wavelengths, λ , at which $R_{rs}(\lambda)$ is generated for the standard OC product. Also shown are the default band pair used in standard processing to derive the aerosol contribution. For PACE OCI, the MBAC algorithm is used where more than 2 bands are utilized as the aerosol bands. Alternative Bands, when available, can also be used to form alternate band pairs for aerosol determination in special circumstances (e.g., very turbid waters), but they are not currently used in the generation of standard products. Note, however, that some of these alternative bands suffer from low signal-to-noise in ocean applications, and some are specifically located in regions of absorbing gas contamination (e.g., 762, oxygen A-band), so they are not well placed for aerosol determination.

Table 4: Sensor-specific center wavelengths, λ , at which $R_{rs}(\lambda)$ is generated for the standard OC product, and the default band pair used in standard processing to derive the aerosol contribution.

Sensor	Rrs Wavelengths (nm)	Aerosol Bands (nm)	Aerosol Bands (nm)
VIIRS	410,443,486,551,671	745,862	1238,1601,2257
SeaWiFS	412,443,490,510,555,670	765,865	
OLI (Landsat-8)	443,482,561,655	865,2201	1609
OLCI	400,412,442,490,510,560,620,665,674,681,709	779,865	754,761,764,885,900,940,1012
OCTS	412,443,490,516,565,667	765,862	
MODIS	412,443,469,488,531,547,555,645,667,678	748,869	859,1240,1640,2130
MERIS	413,443,490,510,560,620,665,681,709	779,865	754,762,885,900
HICO	hyperspectral, 350-1079 by 5.7nm		
GOCI	412,443,490,555,660,680	745,865	
CZCS	443,520,550,670	670	

PACE OCI	hyperspectral, 340-710 by 2.5 nm	750,753,774,777,779,865, 867,870,872,875	1038,1248,1618,21 30,2258
----------	-------------------------------------	---	------------------------------

6. Performance Assessment Validation

6.1. Performance Assessment Validation Methods

After application of the chlor_a algorithms, chlor_a products derived from satellite remote sensing data were validated using in situ data archived in the NASA SeaWiFS Bio-optical Archive and Storage System (SeaBASS; (Werdell et al., 2003)). Following Bailey & Werdell, 2006, the following search criteria were used to find the satellite-in situ matching pairs: sensor zenith angle $<60^\circ$, solar zenith angle $<75^\circ$, 3-hr time difference between in situ and satellite measurements, median value of coefficients of variation (calculated as standard deviation divided by mean) of several products (Rrs between 405 and 570 nm, aerosol optical thickness at 869 nm) $<15\%$ for the 5×5 pixel window centered at the in situ station; $>50\%$ pixels in the 5×5 box must be valid (i.e., not associated with any of the standard quality-control flags such as straylight and high glint).

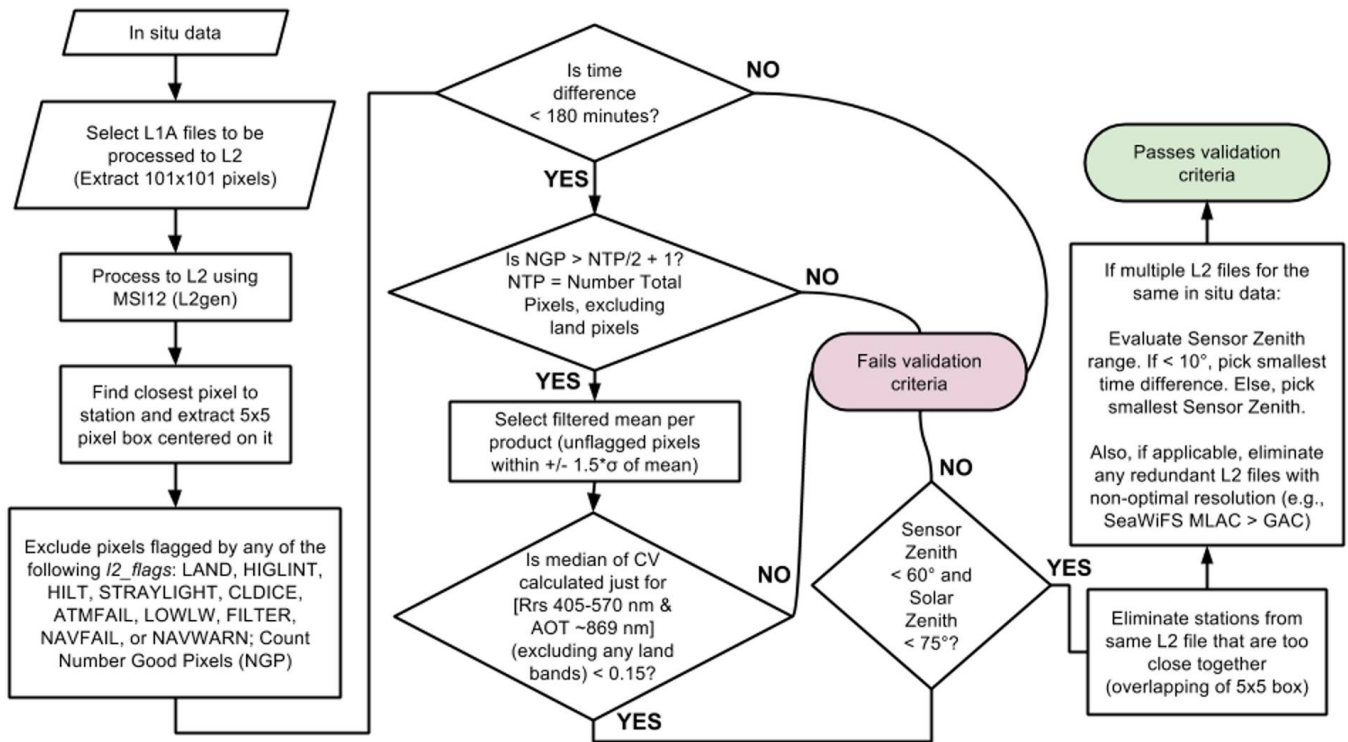


Figure 2: Flowchart of validation processing highlighting the applied exclusion criteria. Adapted and updated from Bailey and Werdell (2006).

This approach of validation is operationally applied by the OBPG to most ocean color sensors. There are a few key recommendations we make from our experience applying the described method to satellite data:

- (1) Use a consistently processed in situ data set
- (2) Eliminate suspect in situ data (e.g. from optically shallow waters) from the validation set
- (3) Use a narrow time window for determining coincidence (i.e. no more than ± 3 h) between in situ and satellite data records
- (4) Use native resolution satellite products (i.e. avoid sub-sampled data)
- (5) Use the mean of a 5×5 pixel box centered on the in situ location
- (6) Appropriately mask satellite pixels on the L2 flags
- (7) Use a homogeneity test (e.g. CV) to minimize the impact of geophysical variability in the 5×5 pixel box on the satellite measurement mean

Following these recommendations will aid in the analysis of the resulting validation results by minimizing the systemic uncertainties.

6.2. Performance Assessment Validation Uncertainties

OBPG produces pixel-level uncertainty products for R_{rs} . Additional references can be found in Zhang et al., (2022 and 2024)Zhang et al., 2022-08Zhang et al., 2024-01.

6.3. Performance Assessment Validation Errors

No content available.

7. Data Access

7.1. Input Data Data Access

7.1.1. Entry #1

URL	https://oceancolor.gsfc.nasa.gov/data/download_methods/
DESCRIPTION	The input variables (rhot, solz, relaz, senz) from level 1 data for R_{rs} production can be downloaded from the ocean color website following the different methods described in the link.

Entry #2

URL	https://oceancolor.gsfc.nasa.gov/resources/docs/ancillary/
DESCRIPTION	The other input variables, including pressure, humidity, wind speed, ozone, water vapor, and NO_2 , are provided as ancillary data in the link above.

7.2. Output Data Data Access

7.2.1. Entry #1

URL	https://oceancolor.gsfc.nasa.gov/data/download_methods/
DESCRIPTION	Rrs and the related output products can be downloaded from the ocean color website following the different methods described in the link.

7.3. Important Related URLs

7.3.1. Entry #1

URL	https://oceancolor.gsfc.nasa.gov/docs/ocssw/atmocer2_8c.html
DESCRIPTION	The graphical description of the algorithm implementation in the NASA ocean color processing code (l2gen).

8. Contacts

Bryan Franz

ROLES	Writing – original draft, Data curation, Visualization, Resources, Investigation, Writing – review & editing, Conceptualization, Formal analysis, Project administration, Funding acquisition, Validation, Methodology, Software, Supervision & Corresponding Author
AFFILIATIONS	NASA Goddard Space Flight Center
EMAIL	bryan.a.franz@nasa.gov
URL	https://science.gsfc.nasa.gov/sed/bio/bryan.a.franz

Amir Ibrahim

ROLES	Writing – original draft, Data curation, Visualization, Resources, Investigation, Writing – review & editing, Formal analysis, Validation,
-------	--

**Methodology, Software, Supervision, Corresponding Author,
Conceptualization, Project administration & Funding acquisition**

AFFILIATIONS

NASA Goddard Space Flight Center

EMAIL

amir.ibrahim@nasa.gov

URL

<https://science.gsfc.nasa.gov/sci/bio/amir.ibrahim>

UUID

0000-0002-3290-056X

References

- Ahmad, Z., Franz, B. A., McClain, C. R., Kwiatkowska, E. J., Werdell, J., Shettle, E. P. & Holben, B. N. (2010). New aerosol models for the retrieval of aerosol optical thickness and normalized water-leaving radiances from the {SeaWiFS} and {MODIS} sensors over coastal regions and open oceans. *Appl. Opt.*, *49*(29), 5545--5560.
- Bailey, S. W., Franz, B. A. & Werdell, P. J. (2010-03). Estimation of near-infrared water-leaving reflectance for satellite ocean color data processing. *Opt. Express*, *18*(7), 7521-7527. <https://doi.org/10.1364/OE.18.007521>
- Bailey, S. W. & Werdell, P. J. (2006). A multi-sensor approach for the on-orbit validation of ocean color satellite data products. *Remote Sensing of Environment*, *102*(1), 12--23.
- Gordon, H. R. & Wang, M. (1994). Influence of oceanic whitecaps on atmospheric correction of ocean-color sensors. *Appl. Opt.*, *33*(33), 7754--7763.
- Ibrahim, A., Franz, B. A., Ahmad, Z. & Bailey, S. W. (2019). Multiband atmospheric correction algorithm for ocean color retrievals. *Frontiers in Earth Science*, *7*, 116.
- Zhai, P., Hu, Y., Trepte, C. R. & Lucker, P. L. (2009-02). A vector radiative transfer model for coupled atmosphere and ocean systems based on successive order of scattering method. *Opt. Express*, *17*(4), 2057--2079. <https://doi.org/10.1364/OE.17.002057>
- Zhang, M., Ibrahim, A., Franz, B. A., Ahmad, Z. & Sayer, A. M. (2022-08). Estimating pixel-level uncertainty in ocean color retrievals from MODIS. *Opt. Express*, *30*(17), 31415-31438. <https://doi.org/10.1364/OE.460735>
- Zhang, M., Ibrahim, A., Franz, B. A., Sayer, A. M., Werdell, P. J. & McKinna, L. I. (2024-01). Spectral correlation in MODIS water-leaving reflectance retrieval uncertainty. *Opt. Express*, *32*(2), 2490--2506. <https://doi.org/10.1364/OE.502561>